



Palladated halloysite hybridized with photo-polymerized hydrogel in the presence of cyclodextrin: An efficient catalytic system benefiting from nanoreactor concept

Samahe Sadjadi¹ | Mohammad Atai²

¹ Gas Conversion Department, Faculty of Petrochemicals, Iran Polymer and Petrochemical Institute, PO Box 14975-112, Tehran, Iran

² Polymer Science Department, Iran Polymer and Petrochemical Institute, PO Box 14975-112, Tehran, Iran

Correspondence

Samahe Sadjadi, Gas Conversion Department, Faculty of Petrochemicals, Iran Polymer and Petrochemical Institute, PO Box 14975-112, Tehran, Iran.

Email: samahesadjadi@yahoo.com; s.sadjadi@ippi.ac.ir

Mohammad Atai, Polymer Science Department, Iran Polymer and Petrochemical Institute, PO Box 14975-112, Tehran, Iran.
Email: m.atai@ippi.ac.ir

Considering the excellent performance of halloysite as a catalyst support and in an attempt to benefit from the concept of nanoreactors in the catalysis, an innovative catalytic system has been designed, in which acrylamide and bis-acrylamide were photo-polymerized in the presence of palladated halloysite. The novel precipitation photo-polymerization method avoided the formation of an extended polymeric network, but led to the formation of co-polymer on the halloysite periphery. The co-polymer exhibited good swellability in aqueous media and formed hydrogel. This hydrophilic environment around catalytic palladated halloysite can be considered as a nanoreactor that can concentrate the substrate and bring them into the vicinity of the palladated halloysite. This catalytic system was used for promoting hydrogenation of hydrophobic nitro arenes in aqueous media. To avoid immiscibility of hydrophobic substrates and hydrophilic nature of the nanoreactor, that emerged from swelling of hydrogel, β -cyclodextrin (CD) was utilized as phase transfer agent. The results confirmed high catalytic activity of this catalytic system. Even highly hydrophobic substrates could tolerate hydrogenation under this protocol to furnish the corresponding product in high yield. Finally, the contribution of both CD and hydrogel to the catalysis was confirmed. Moreover, studying the recyclability of the catalyst as well as Pd leaching proved the high recyclability of the catalyst and low leaching of Pd nanoparticles.

KEYWORDS

catalyst, halloysite, hydrogel, hydrogenation, photo-polymerization

1 | INTRODUCTION

Hydrogenation of nitro arenes to the corresponding anilines is one of the most important hydrogenation reactions, mostly catalyzed in the presence of Pd-based catalysts.^[1–4] As Pd is one of the precious metals, its recovery and recycling are economically important. To decrease the required amount of Pd and facilitate its recovery, heterogenation of Pd by using heterogeneous supports is suggested.^[5–11]

One of the mostly used oligosaccharides for catalytic purposes is β -cyclodextrin (β -CD). The extensive use of this compound is due to its unique conical scaffold that provides a hydrophobic cavity and hydrophilic exterior, biocompatibility, non-toxic nature, and cost-effectiveness.^[12] The remarkable feature of CD that allows development of environmentally benign procedures in aqueous media is its capability for embedding hydrophobic substrates and transferring them to the aqueous media.^[13–16] Taking advantage of this

feature, various aqueous biphasic catalysts have been developed.^[17,18]

Use of clays as supports for immobilization of the catalytic species and development of heterogeneous catalyst is well established.^[19] In this line, the utility of naturally occurring biocompatible halloysite nanoclay, Hal, that is a dioctahedral 1:1 layered aluminosilicate $[\text{Al}_2\text{Si}_2\text{O}_5(\text{OH})_4 \cdot n\text{H}_2\text{O}]$ has attracted growing attention, and recently many Hal-based heterogeneous (photo) catalysts with outstanding catalytic performances have been reported.^[20–22] It is worth noting that apart from individual Hal, various Hal-based hybrid systems have also been designed and applied for catalytic purposes.^[23–25] Notably, the physical and chemical features of Hal such as tubular morphology, high chemical and mechanical stability, inert and non-toxic nature, oppositely charged inner and outer surface, and the capability of surface functionalization render Hal a promising clay not only in the field of catalysis, but also for many scientific domains such as drug delivery, composites and polymer science.^[25–40]

Hydrogels are water-swallowable synthetic or natural 3D crosslinked hydrophilic polymeric networks with high biocompatibility and mechanical strength. These soft and porous polymeric materials that mostly contain the hydrophilic moieties such as hydroxyl, sulfonic, carboxylic and amidic functional groups can swell in aqueous media. However, they are not water soluble due to their physical and/or chemical properties. Hydrogels are extensively used in a diverse range of applications, ranging from chemical separation to biomedical engineering and drug delivery systems.^[41–43]

There are a few reports on the Hal-hydrogel composites, mostly used for controlled release,^[41] reinforcement of hydrogel^[43] and soft tissue engineering.^[42] To the best of our knowledge, there is only one report on the catalytic application of Hal-hydrogel, in which the covalent hybrid of thermo-responsive poly(*N*-isopropylacrylamide) (PNIPAAm) and Hal was used for the immobilization of Pd nanoparticles and development of Hal-PNIPAAm/PdNPs as a catalyst for the Suzuki reaction.^[25] It was believed that due to the hydrophilic nature of the swelled form of the hydrogel at lower temperature (temperatures lower than the lower critical solution temperature) it was unsatisfactory for hydrophobic substrates, and superior catalytic activity was achieved at elevated temperature.

Following our study on the Hal-based heterogeneous catalyst,^[23] recently we have developed hybrid systems composed of Hal and CD. The study of the catalytic activity of these hybrid systems proved that they could benefit from the chemistry of both components, and the presence of CD as a phase transfer agent could increase the rate of the reactions in aqueous media.^[23,24,44]

Taking these results into account and considering the fact that despite the presence of hydroxyl groups on the surface of Hal, it still has a relatively weak adhesion with Pd nanoparticles due to the absence of chemical interaction,^[19,27] design and preparation of a novel Hal-hydrogel catalytic system for hydrogenation of nitro arenes was targeted. It is assumed that the polymeric functionality on Hal not only can result in efficient immobilization of Pd nanoparticles due to the electrostatic reactions of Pd nanoparticles with many amide functionalities on the polymer backbone, but also the nano-environment aroused from polymer swelling in aqueous media could effectively concentrate the substrates and enhance the reaction rate. To circumvent the immiscibility of hydrophobic substrates and hydrophilic nature of the nanoreactor and allow the reactions to be carried out in aqueous media at low temperature, CD was used as a phase transfer agent. To prepare the catalyst, Hal was first functionalized with 3-(trimethoxysilyl) propyl methacrylate and then used for immobilization of Pd nanoparticles to furnish Pd/Hal-V. Subsequently, acrylamide (AAM) and bisacrylamide (BisAAM) were co-polymerized in the presence of Pd/Hal-V via a novel procedure, precipitation photo-polymerization. On the contrary of conventional co-polymerization methods that led to the formation of an extended polymeric network, precipitation photo-polymerization could control the co-polymerization process in a way that the co-polymer was formed on the periphery of Pd/Hal-V. The catalytic activity of the resulting hybrid, Pd/Hal-H, in the presence of β -CD as a co-catalyst, was examined for hydrogenation of nitro arenes. To establish the contribution of hydrogel and CD in the catalysis, several model catalysts were prepared, and their catalytic activities compared with that of the catalyst. Moreover, the recyclability of the catalyst as well as Pd leaching were investigated.

2 | EXPERIMENTAL

2.1 | Instruments

To characterize the catalyst, Brunauer–Emmett–Teller analysis, thermogravimetric analysis (TGA), field emission scanning electron microscopy (FE-SEM), transmission electron microscopy (TEM), X-ray diffraction (XRD), Fourier transform-infrared spectroscopy (FT-IR) and inductively coupled plasma-atomic emission spectroscopy (ICP-AES) were employed. To record TEM images of the catalyst and estimate the average Pd particle sizes, Tecnai microscope (200 kV) was used. For this analysis, the catalyst was dispersed in water and, after

evaporation of the solvent, the TEM images were recorded. The apparatus used for recording FE-SEM was MIRA3 TESCAN. The structure of the catalyst was studied by using XRD (Siemens, D5000, Cu K α radiation from a sealed tube). Moreover, the XRD pattern of the catalyst was compared with that of the pristine Hal. To verify formation of the catalyst and studying the effect of the recycling on the structure of the catalyst, the FT-IR spectra (Spectrum 65, Perkin-Elmer) of the pristine Hal, and fresh and recycled catalysts were recorded and compared. To study the thermal stability of the catalyst and measuring the content of polymer and organosilane, TGA (Mettler Toledo) was performed under N₂ atmosphere by using a heating rate of 10°C min⁻¹. The textural properties of the catalyst were studied by recording N₂ adsorption-desorption isotherm using BELSORP Mini II apparatus. To perform this analysis, the catalyst was pre-heated at 200°C for 3 hr. Finally, Pd loading and leaching of the catalyst were calculated using the ICP-AES method (Varian, Vista-pro).

2.2 | Materials and methods

2.2.1 | Materials

The chemicals used for synthesis of the catalyst and performing hydrogenation reaction included AAM and BisAAM, obtained from Merck (Germany); Hal, nitro arenes, camphorquinone (CQ), dimethyl aminoethyl methacrylate (DMAEMA), 3-(trimethoxysilyl) propyl methacrylate, Pd (OAc)₂, NaBH₄, MeOH and toluene, purchased from Sigma-Aldrich (Germany).

2.2.2 | Surface functionalization of Hal with 3-(trimethoxysilyl) propyl methacrylate: Hal-V

Initially, surface modification of Hal was carried out through our previously reported procedure.^[24] Briefly, 3-(trimethoxysilyl) propyl methacrylate (4 mL) was added to the well-dispersed suspension of Hal (2.5 g) in dry toluene (50 mL). The resulting mixture was then refluxed at 110°C overnight. Upon completion of the reaction, the precipitate was filtered off, washed several times with dried toluene and dried at 90°C overnight.

2.2.3 | Immobilization of Pd nanoparticles: Pd/Hal-V

Immobilization of Pd nanoparticles on the surface of Hal-V was simply accomplished via the wet impregnation

method. Typically, to a stirring suspension of Hal-V (1.2 g) in dry toluene (15 mL), Pd (OAc)₂ (0.02 g) was slowly added and the resulting mixture was vigorously stirred at ambient temperature for 10 hr. The reduction of Pd (II) to Pd (0) was carried out by using NaBH₄ as reducing agent. More precisely, a mixture of NaBH₄ in toluene and methanol (10 mL, 0.2 N) was added to the suspension of Pd (II)-Hal-V in a dropwise manner, and the resulting mixture was stirred for 5 hr. After that, the black solid was filtered, washed with methanol repeatedly and dried in the oven at 80°C overnight.

2.2.4 | Optimization of initiator concentration

To find the optimum initiator concentration for the photo-polymerization of AAM, different concentrations of 0.5, 1.0, 1.5 and 2 wt.% of CQ and DMAEMA were used as photoinitiator system in the AAM solution. The results showed an increase in the conversion of the AAM by increasing the initiator concentration up to 1 wt.% with no further increase in the conversion upon enhancing the initiator concentration. Therefore, further experiments were performed using CQ and amine at a concentration of 1 wt.% .

2.2.5 | Optimization of concentration of the crosslinker

To optimize the concentration of the crosslinker in the polymerization system, BisAAM was incorporated in concentrations of 1, 2, 3, 4 and 5 wt.% in the monomer solution. Having polymerized the AAM and the crosslinking agent, the product was washed with acetone and dried, and its swelling behavior in de-ionized (DI) water was then examined. It was found that the specimens containing the crosslinker up to 2 wt.% were easily swollen in the water forming a very-low-strength hydrogel. At concentrations of 4 wt.% and higher, the reaction resulted in a polymer network with high crosslink density, which hardly swelled in DI water. The water uptake of the crosslinked PAAm specimens containing 2, 3, 4 and 6% BisAAM as crosslinker are summarized in Table 1.

The crosslinker at 3 wt.% resulted in a hydrogel with high water sorption and a discrete structure that is desirable as a substrate for the catalyst. Therefore, the catalyst (palladium-containing hydrogel) was prepared using 3 wt.% BisAAM as crosslinker.

TABLE 1 The water uptake of the crosslinked PAAM specimens containing 2, 3, 4 and 6 wt.% BisAAM as crosslinker was determined according to the method described in Section 2.2.6

BisAAM wt. %	2	3	4	6
Water uptake (%)	Could not be measured as the polymer in water formed a continuous sticky and mostly sol structure. The structure is not suitable as a substrate for the catalyst.	730	460	400

BisAAM, bis-acrylamide.

2.2.6 | Precipitation photo-polymerization of AAM: Synthesis of Pd/Hal-H

A solution of 25 wt.% of AAM monomer in acetone was prepared; 3 wt.% of BisAAM (based on the AAM monomer) as crosslinking agent and 20 wt.% of Pd/Hal-V (based on the AAM monomer) were added to the solution. The suspension was stirred for 1 hr, and then ultra-sonicated (20 kHz, 100 W) for 10 min with intervals of 7 s on and 3 s off. Then, 1 wt.% CQ and 1 wt.% DMAEMA (both based on the AAM monomer) were added to the suspension in the dark. The mixture was then inserted into a glass reactor equipped with condenser and mechanical stirrer. The solution in the reactor was then irradiated using a homemade blue light source for 30 min. The light source consisted of LED lamps with emission wavelength of 470 (± 5) nm and power of 50 W (Figure 1). The reactor was irradiated on both sides having applied the light sources while the solution was stirring. Considering the fact that acetone is a good solvent for AAM and BisAAM but a non-solvent for their copolymer, the polymer chains are precipitated as the reaction is progressed.

Upon completion of the reaction, the precipitated solid was washed with fresh acetone and centrifuged to separate the Pd/Hal-H. The washing and centrifugation were repeated three times to remove any unreacted monomer, crosslinker and initiator system. The polymer was then dried and used for further investigation. The process of synthesis of the catalyst has been schematically presented in Figure 2.

The content of Pd in the structure of the catalyst was calculated using ICP-AES analysis. The procedure for preparing ICP sample included digestion of organic moiety through treatment of a known amount of the catalyst with concentrated acid solution (mixture of concentrated nitric and hydrochloric acids). Using this methodology, the content of Pd was estimated to be 0.1 wt.%.

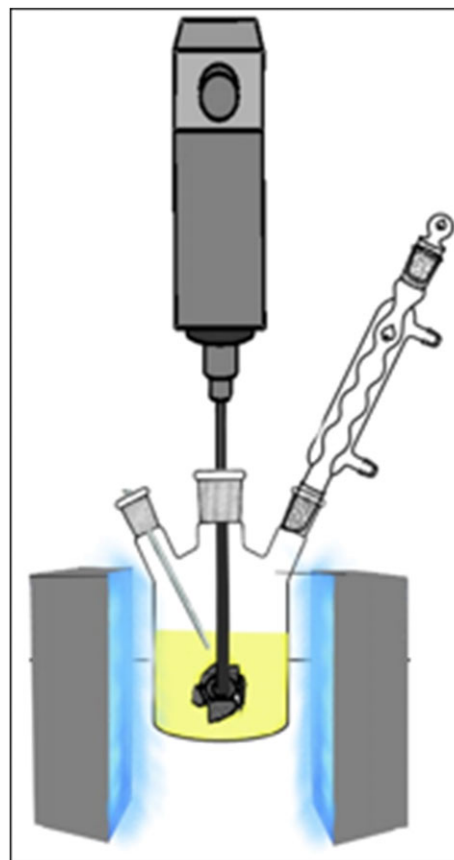


FIGURE 1 The photo-polymerization reaction set up

2.2.7 | General procedure for the hydrogenation of nitro arenes

Typically, nitro arene (1 mmol), CD (1 wt. %) and catalyst (2 wt. %) were placed in DI water (2 mL). The reaction mixture was then heated up to 50°C, and then H₂ gas (1 bar) was purged into the glass reactor under stirring. The progress of the reaction was traced by using thin-layer chromatography. Upon completion of the reaction, the catalyst was filtered off and the corresponding amine product was achieved by evaporating water. Considering the fact that all the products were previously reported, their identification was carried out by comparing boiling/melting points and FT-IR spectra with those of the authentic sample. To recycle the catalyst, the recovered catalyst was washed with water and dried at 90°C overnight.

2.2.8 | Catalyst water uptake

To determine the catalyst swelling ratio in water (water uptake), 0.01 g of the catalyst was placed in a jar and 10 g DI water was added to it. After 24 hr the excess water

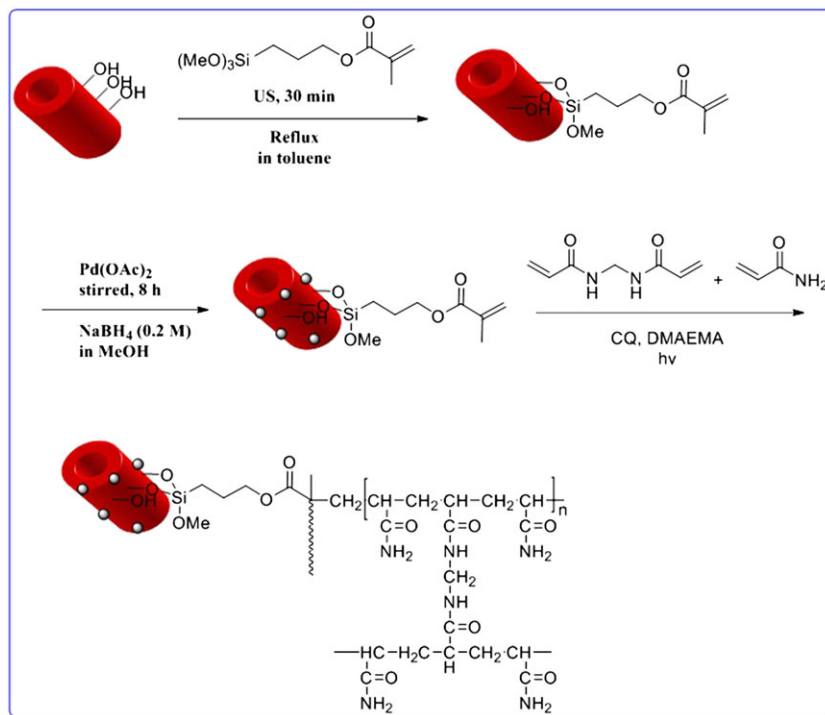


FIGURE 2 The schematic procedure for the synthesis of the catalyst

was removed by filter paper and the water uptake was calculated as follows:

$$\text{water uptake (wt.\%)} = \frac{w_1 - w_0}{w_0} \times 100$$

where w_0 is the initial weight of the catalyst and w_1 is the weight of the swollen catalyst after removal of excess water.

3 | RESULTS AND DISCUSSION

3.1 | Catalyst characterization

Initially, the FT-IR spectra of Pd/Hal-H and Hal-V were recorded and compared with that of pristine Hal (Figure 3). As the comparison of the three FT-IR spectra reveals, the Hal characteristic bands, i.e. the bands at 1033 cm^{-1} (Si-O stretching), 540 cm^{-1} (Al-O-Si vibration), 3697 cm^{-1} and 3624 cm^{-1} (internal -OH groups), 1645 and 2923 cm^{-1} ^[28] are observed in the FT-IR spectra of both Pd/Hal-H and Hal-V, indicating that the Hal structure is preserved upon incorporation of the silane group and polymer. Notably, the FT-IR spectrum of Hal-V is very similar to that of pristine Hal. This issue can be attributed to the low content of V on the Hal-V hybrid (as confirmed by TG analysis, vide infra). Moreover, most of the characteristic bands of V (i.e. the bands related to the -C=C and -Si-O) overlapped with those of Hal. However, a small band at 1734 cm^{-1} can be detected

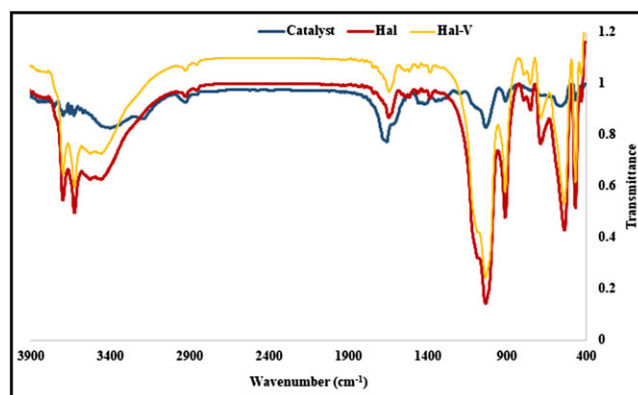


FIGURE 3 Fourier transform-infrared (FT-IR) spectra of pristine Hal, Hal-V and the catalyst

that can be assigned to -C=O functionality. It is worth noting that in the FT-IR spectrum of the catalyst the intensities of the Hal characteristic bands decreased. Moreover, an additional band at 1690 cm^{-1} is seen that can be assigned to the amidic carbonyl groups in the polymeric network.

To further characterize the structure of Pd/Hal-H, the XRD pattern of the catalyst was obtained and compared with that of pristine Hal (Figure 4). The XRD pattern of Hal is well established, and shows peaks at $2\theta = 12^\circ$, 19.9° , 24.7° , 26.6° , 35.1° , 38.3° , 55° and 62.7° (JCPDS No. 29-1487).^[45,46] As depicted, the characteristic peaks of Hal can also be detected in the XRD pattern of the catalyst. However, their intensities are decreased. It is worth

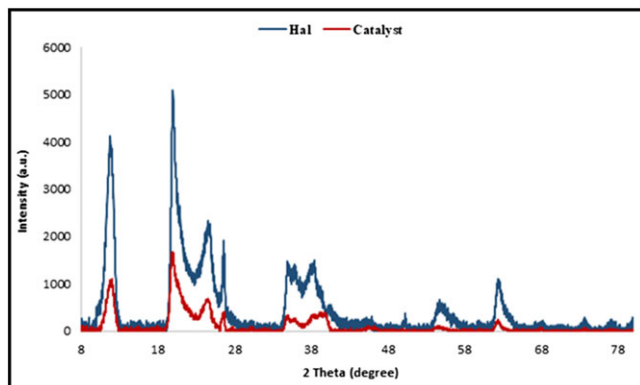


FIGURE 4 X-ray diffraction (XRD) patterns of pristine Hal and the catalyst

noting that no significant shift or change of the interlayer distance was observed in the XRD pattern of Pd/Hal-H compared with that of pristine Hal, implying that the polymeric chains were grown on the surface of Hal and form the crosslinked network. It is worth noting that in the XRD pattern of the catalyst the characteristic peaks of Pd nanoparticles were not observed. According to the literature,^[47] the low content of Pd (as confirmed via ICP analysis) and its high distribution can justify this observation.

Next, the morphology of Pd/Hal-H was studied by recording the TEM and FE-SEM images. According to the literature, in which composite of Hal and hydrogel was synthesized via conventional polymerization method,^[41] Hal was dispersed in a vast polymeric network. In this work, as the used amount of the Pd/Hal-V

in the course of synthesis of the catalyst was only 20 wt.%, it was expected that similar to previous reports Pd/Hal-V was entrapped within the polymeric network. However, both FE-SEM and TEM images (Figures 5 and 6) revealed that using the photo-polymerization procedure, the polymeric network was formed just on the periphery of the Pd/Hal-V tubes. More precisely in both images, the Hal tubes are observable as the main

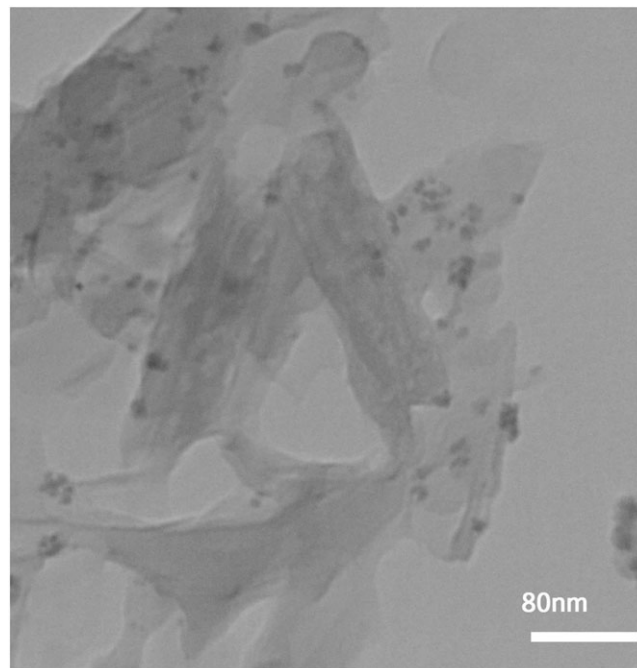


FIGURE 6 Transmission electron microscopy (TEM) images of the catalyst

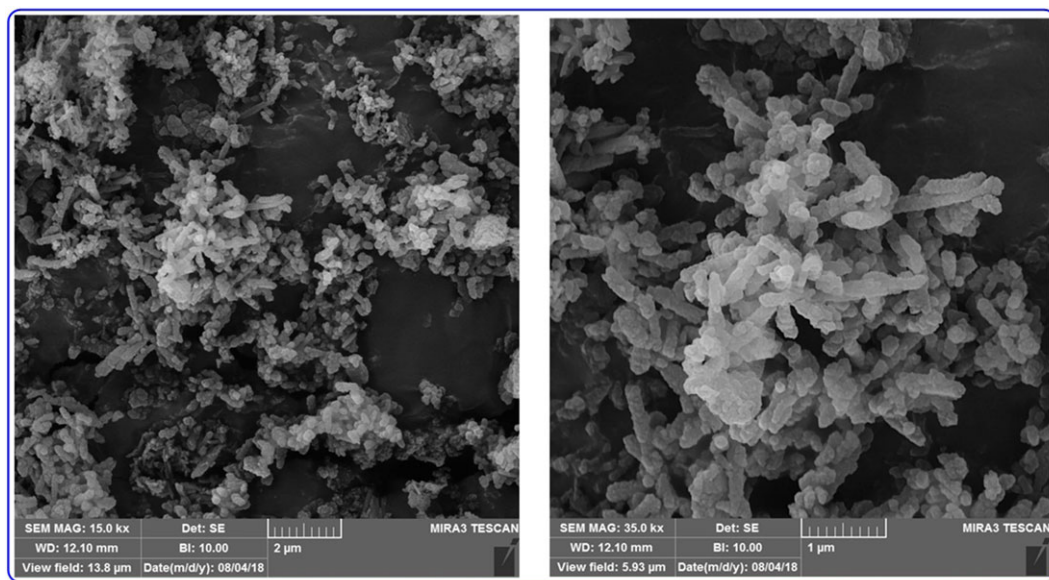


FIGURE 5 The field emission scanning electron microscopy (FE-SEM) images of the catalyst

morphology and the polymers are detected around the tubes. In other word, in the SEM and TEM images of the catalyst an extended polymeric network was not seen. This observation can be attributed to the use of the photo-polymerization procedure in the presence of Pd/Hal-V. In detail, Pd/Hal-V that is a grayish powder can absorb the light and reduce the yield of the photo-polymerization reaction. On the other hand, the photo-polymerization reaction time was low. Hence, the reaction time and condition prevented from formation of an extended polymeric network. Notably, in the TEM image of the catalyst the Pd nanoparticles are observable. Using TEM images, the average Pd particle size was estimated to be 5 nm.

To estimate the content of the polymer on the structure of the Pd/Hal-H and study its thermal stability, TG analysis was exploited. In Figure 7, the thermogram of the catalyst is illustrated and compared with that of pristine Hal and Hal-V.

The thermogram of pristine Hal is in good accord with the literature,^[48,49] and exhibited two main weight losses, one (~150°C) assigned to loss of water and another one (~550°C) related to Hal dehydroxylation. The thermogram of Hal-V also shows the above-mentioned weight losses. Furthermore, an additional weight loss (~3 wt.% at about 300°C) is observable that can be assigned to the degradation of organosilane.

Similarly, the thermogram of the catalyst exhibits the weight losses of pristine Hal. Moreover, additional weight losses related to the organosilane and polymer are detectable.

According to the thermogram of Hal, about 82.3 wt.% of the pristine Hal remains at 800°C, and the remaining ash in the thermogram of the catalyst is 37.7 wt.%. The polymer percentage of the catalyst is then calculated as follows:

$$\begin{aligned} &\text{Polymer percentage in in the catalyst} \\ &= (100 - 37.7/82.3 * 100) = 54.2 \text{ wt.}\% \end{aligned}$$

Finally, the nitrogen adsorption–desorption isotherm of Pd/Hal-H was recorded to study how hybridization with hydrogel can affect the surface properties of Hal. The results confirmed the similarity of the isotherm of Pd/Hal-H (Figure 8) with that of the pristine Hal (Figure S1). More precisely, both isotherms showed type II isotherms with H3 hysteresis loops.^[46] The comparison of the specific surface area of pristine Hal ($51 \text{ m}^2 \text{ g}^{-1}$) with Pd/Hal-H showed that upon introduction of polymer on the surface of Hal, the specific surface area did not change significantly (the specific surface area of the catalyst was $54 \text{ m}^2 \text{ g}^{-1}$). This observation can be due to the porous nature of the polymer. Moreover, the total pore volume of the catalyst (12.4 cm^3) was slightly higher than that of pristine Hal (11.7 cm^3). On the other hand, the pore diameter of the catalyst (28.6 nm) was remarkably larger than that of pristine Hal (5.4 nm). This observation can show that on the polymeric network both large and small pores are present. Totally, it seems precipitated polymers on the halloysite substrate provide higher porosity on the surface of the nanoparticles.

The measurement of the water swelling of the catalyst showed a water uptake of 750 wt.% based on the catalyst, which would be about 1380 wt.% based on the polymer part of the catalyst.

It is worth noting that in this work precipitation photo-polymerization was used as a fast procedure for formation of polymer. As in the method, the polymer is precipitated

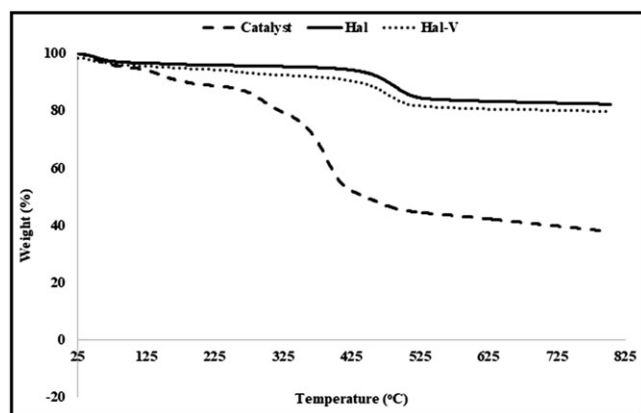


FIGURE 7 The thermogravimetric analyses (TGA) of pristine Hal, Hal-V and the catalyst

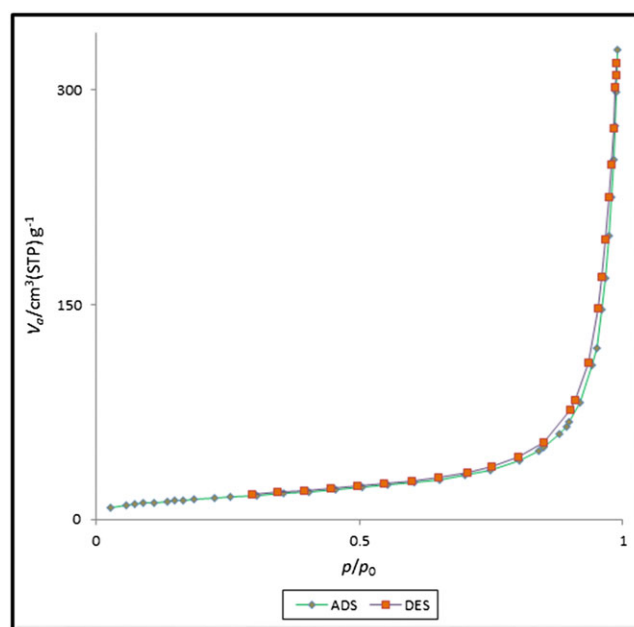


FIGURE 8 N₂ adsorption–desorption isotherm of the catalyst

from solvent and is easily separated from the polymerization medium, which significantly facilitates the work-up step. Furthermore, the method provides a porous texture on the catalyst substrate, which is of great importance for the catalytic activity of the final catalyst. Under conventional polymerization methods, Hal is entrapped within the hydrogel network,^[41] while in the precipitation photo-polymerization method the formation of hydrogel can be controlled in a way that it can only be formed around the Hal tube (as confirmed by TEM). The reason for employing the photo-polymerization method was the fact that the preliminary catalytic experiments showed low catalytic activity of Pd/H (vide infra). Moreover, the accessibility of the substrates to the catalytic active sites could be limited in a catalyst in which Hal was dispersed in an extended and bulky hydrogel network.

3.2 | Catalytic activity

To initiate the studies of the catalytic performance of the catalytic system and the role of hydrogel and CD in the catalysis, two control catalysts, including Pd/Hal-V (see SI) and Pd/H, with similar Pd contents were synthesized (see SI, Figures S2 and S3). Moreover, one hydrogenation reaction, hydrogenation of nitrobenzene, was selected as a model reaction and the optimization of the reaction condition was carried out (see SI). Subsequently, the comparison of the catalytic activity of Pd/Hal-V, Pd/H and Pd/Hal-H in the presence and absence of CD was accomplished (Table 2). As tabulated in Table 2, in all cases, addition of CD led to a significant increase in product yield. This observation confirms the probability of formation of an inclusion complex between CD and

hydrophobic substrates. More precise comparison of the catalytic activities of the catalysts showed that the catalytic activity of the catalyst (Pd/Hal-H) was the highest compared with that of Pd/Hal-V and Pd/H. As the contents of Pd in all catalysts were similar and both H and Hal were hydrophilic, the superior catalytic activity of Pd/Hal-H can indicate the possible synergism between H and Hal.^[24]

The comparison of entries 6 and 7, in which different amounts of CD were used as co-catalyst, implies that only a low amount of CD (1 wt.%) was adequate for promoting the reaction, and further increasing this value to 2 wt.% did not affect the yield of the reaction.

Next, the effect of Pd content of the catalyst on the catalytic activity of the catalyst was investigated by preparing the catalysts with different loading of Pd ranging from 0.03 to 0.2 wt.% (samples with 0.03, 0.1, 0.2 wt.%), and the comparison of the catalytic activities of the samples with that of the catalyst showed that there was not a linear relationship between the Pd content of the catalyst and the observed catalytic activity, and the best result was achieved with the catalyst with 0.1 wt.% Pd. As Pd nanoparticles are the main catalytic species for hydrogenation, the lower catalytic activities of the catalysts with lower content of Pd than 0.1 wt.% were attributed to the lack of catalytic active sites for promoting the reaction. In the case of catalysts with higher content of Pd that showed lower catalytic activities, it was assumed that use of a higher amount of Pd could lead to aggregation of the Pd and a decrease in the catalytic activity. To verify this assumption, the TEM images of that sample were recorded (Figure S4) and compared with that of the catalyst. The comparison of the average Pd particle sizes indicated the aggregation of Pd nanoparticles in the case of use of higher content of Pd, confirming the importance of the average Pd particle size on the catalysis.

In the following, to elucidate whether this catalyst is selective toward the nitro group and whether this protocol can be generalized to the steric and highly hydrophobic substrates, hydrogenation of two more substrates, highly hydrophobic 1-nitronaphthalene and 4-nitroacetophenone, that possess two functional groups was investigated (Table 3). As illustrated, the reactivity of the substrates follows the order of 4-nitroacetophenone > nitrobenzene > 1-nitronaphthalene. The lower catalytic activity observed in the case of 1-nitronaphthalene can be attributed to its steric nature. In other words, the encapsulation of this substrate into the cavity of CD and formation of the inclusion complex is more tedious than small substrates; hence, phase transferring to the aqueous media is retarded and lower yield of the desired product is furnished. As shown, two other substrates, nitrobenzene and 4-nitroacetophenone,

TABLE 2 The efficiency of various catalytic systems for hydrogenation of nitrobenzene^a

Entry	Catalyst	Catalyst amount (wt.%)	CD amount (wt.%)	Time (hr)	Yield (%) ^b
1	Pd/Hal-V	2	–	2	30
2	Pd/Hal-V + CD	2	1	2	60
3	Pd/H	2	–	2	40
4	Pd/H + CD	2	1	2	63
5	Pd/Hal-H	2	–	2	60
6	Pd/Hal-H	2	1	2	95
7	Pd/Hal-H	2	2	2	95

^aReaction condition: substrate (1 mmol), catalyst, H₂O (2 mL), hydrogen flow of 50 mL min⁻¹, agitation (800 rpm) at 50°C in 1 hr.

^bIsolated yields.

CD, cyclodextrin.

TABLE 3 Hydrogenation of nitro compound under Pd/Hal-H+ CD catalysis^a

Entry	Substrate	Amount of cat. (wt.%)	Amount of CD (wt.%)	In the presence of CD		Without CD	
				Time (hr)	Yield (%) ^b	Time (hr)	Yield (%) ^b
1	Nitrobenzene	2	1	2	95	2	60
2	1-Nitronaphthalene	2	1	3	85	3	60
3	4-Nitroacetophenone	2	1	3	98	3	70

^aReaction condition: substrate (1 mmol), catalyst (2 wt.%), H₂O (2 mL), hydrogen flow of 50 mL min⁻¹, agitation (800 rpm) at 50°C.

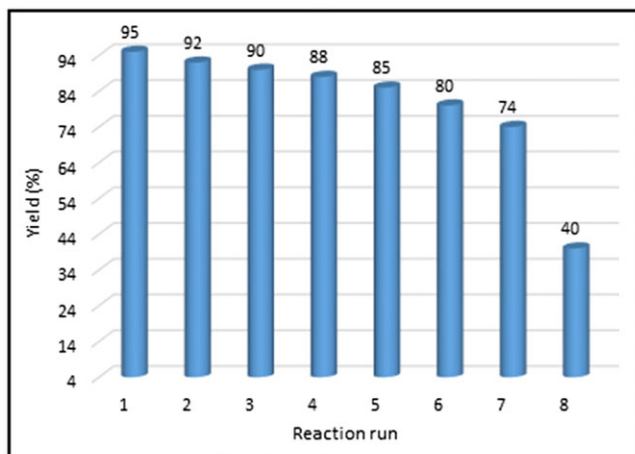
^bIsolated yields.

CD, cyclodextrin.

exhibited comparative yields, indicating that the presence of other comparative functional groups (i.e. carbonyl) on the aromatic ring did not affect the catalytic activity and the catalyst was totally selective toward the nitro group and hydrogenation of the carbonyl group did not take place.

3.3 | Catalyst recyclability

The final features of the catalyst that were studied were catalyst recyclability and Pd leaching. As described in the Experimental section, after completion of the first reaction run of hydrogenation of nitrobenzene, the catalyst was separated, washed and dried. Then, the recovered catalyst was applied for promoting the next run of the reaction under similar reaction conditions. The recycling was repeated for eight consecutive reaction runs, and the yield of aniline (model product) for each cycle was measured and compared with that of fresh catalyst. In Figure 9, the results of recycling experiments are presented. As depicted, for the first five recycling experiments, the catalyst showed high recyclability and catalytic activity decreased by only 10%. Upon further

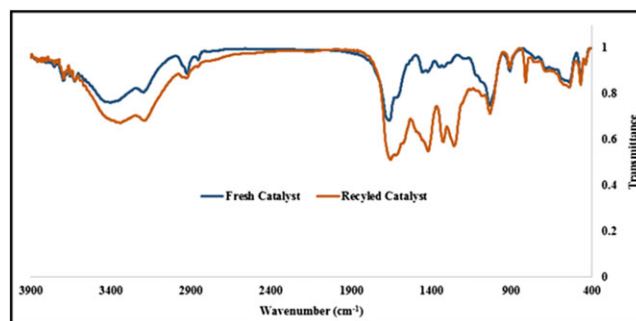
**FIGURE 9** The results of catalyst recyclability

recycling, however, the slope of the loss of catalytic activity was higher and, upon the eighth recycling, significant catalytic activity loss was observed.

To elucidate whether the catalyst preserved its structure in the course of recycling, the FT-IR spectrum of the recycled Pd/Hal-H was recorded (Figure 10). As depicted in Figure 10, the FT-IR spectrum of the recycled catalyst showed the characteristic bands of the fresh one. This observation indicated that the structure of the catalyst was not diminished in the course of recovery and recycling. However, as can be seen in Figure 10, the intensities of the bands in two peaks are different, and some broadening is observed in the FT-IR spectrum of the recycled catalyst.

Next, the Pd leaching of Pd/Hal-H was measured by using ICP. It is worth noting that the leaching of the Pd nanoparticles for the first five runs of the reaction was negligible (2.3 wt.% Pd content of the catalyst) and then slowly increased, and upon the eighth recycling significant Pd leaching (5.7 wt.% Pd content of the catalyst) was observed.

Finally, the TEM analysis of the recycled catalyst was performed to elucidate whether recycling could provoke any change in the morphology and Pd particle size (Figure 11). As shown in Figure 11, the Hal tubes in the recycled catalyst are observable and the morphology of the catalyst is similar to that of the catalyst. Hence, it can be concluded that recycling did not cause significant

**FIGURE 10** The comparison of the Fourier transform-infrared (FT-IR) spectra of fresh and recycled catalyst

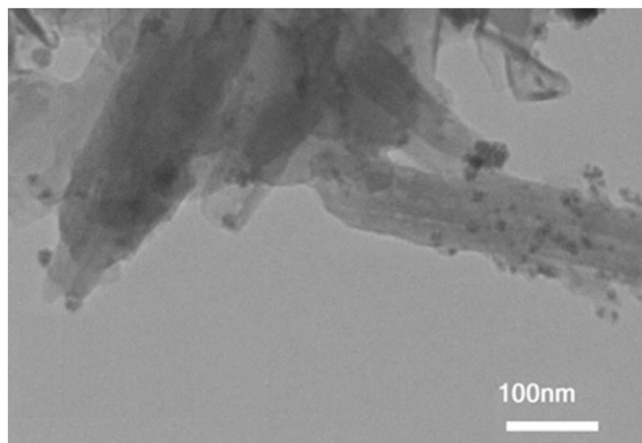


FIGURE 11 Transmission electron microscopy (TEM) image of the recycled catalyst

morphology change. Regarding the Pd nanoparticle average size, it was found that recycling several times could lead to slight aggregation of Pd nanoparticles and an increase of Pd particle size to 8 nm.

4 | CONCLUSION

Taking advantage of the swellability of hydrogels that form a hydrophilic nano-environment and the capability of CD for formation of inclusion complex with hydrophobic substrates and serving as a phase transfer agent, as well as the high performance of Hal, a novel catalytic system was prepared through precipitation photopolymerization of AAM and BisAAM in the presence of palladated halloysite. The characterization of the catalyst confirmed that using the photo-polymerization method, a polymeric sheath was formed on the surface of Hal that highly swelled in water. Investigation of the catalytic activity of the catalyst for the hydrogenation of nitroarenes in the presence of CD as phase transfer agent confirmed the high activity and selectivity of the catalyst. Moreover, the contribution of both hydrogel and CD to the catalysis was proved. Notably, Pd/Hal-H exhibited high recyclability and low Pd leaching.

ACKNOWLEDGEMENT

The authors appreciate partial financial supports from Iran Polymer and Petrochemical Institute. S.S. fully appreciates Prof. Heravi's support.

CONFLICT OF INTEREST

There are no conflicts to declare.

ORCID

Samahe Sadjadi  <https://orcid.org/0000-0002-6884-4328>

REFERENCES

- [1] T. Sugimura, K. Wakabayashi, H. Nakagama, M. Nagao, *Cancer Sci.* **2004**, *95*, 290.
- [2] H. U. Blaser, C. Malan, B. Pugin, F. Spindler, H. Steiner, M. Studer, *Adv. Synth. Catal.* **2003**, *345*, 103.
- [3] M. Cargnello, V. V. T. Doan-Nguyen, T. R. Gordon, R. E. Diaz, E. A. Stach, R. J. Gorte, P. Fornasiero, C. B. Murray, *Science* **2013**, *341*, 771.
- [4] G. Sevjidsuren, S. Zils, S. Kaserer, A. Wolz, F. Ettingshausen, D. Dixon, A. Schoekel, C. Roth, P. Altantsog, D. Sangaa, C. Ganzori, *J. Nanomater.* **2010**, *2010*, 1.
- [5] P. G. N. Bouchenafa-Saib, P. Verhasselt, F. Addoun, V. Dubois, *Appl. Catal. A Gen.* **2005**, *286*, 167. *Appl. Catal. A Gen.* **2005**, *286*, 167
- [6] X. Yu, M. Wang, H. Li, *Appl. Catal. A Gen.* **2000**, *202*, 17.
- [7] R. Giordano, P. Serp, P. Kalck, Y. Kihn, J. Schreiber, C. Marhic, J.-L. Duvail, *Eur. J. Inorg. Chem.* **2003**, *2003*, 610.
- [8] C.-H. Li, Z.-X. Yu, K.-F. Yao, S.-F. Ji, J. Liang, *J. M. Cat. A Chem.* **2005**, *226*, 101.
- [9] P. Sangeetha, K. Shanthi, K. S. Rama Rao, B. Viswanathan, P. Selvam, *Appl. Catal. A Gen.* **2009**, *353*, 160.
- [10] N. Arora, A. Mehta, A. Mishra, S. S. Basu, *App. Clay Sci.* **2018**, *151*, 1.
- [11] Y. Chen, L. Li, L. Zhang, J. Han, *Colloid Polymer Sci.* **2018**, *296*, 567.
- [12] S. Manivannan, R. Ramaraj, *Chem. Eng. J.* **2012**, *210*, 195.
- [13] S. Noël, B. Légera, A. Ponchel, F. Hapiot, E. Monflier, *Chem. Eng. Trans.* **2014**, *37*, 337.
- [14] L. Bai, F. Wyrwalski, J. F. Lamonier, A. Y. Khodakov, E. Monflier, A. Ponchel, *Appl. Catal. B* **2013**, *381*, 138.
- [15] A. Gogoi, K. C. Sarma, *Mater. Chem. Phys.* **2017**, *194*, 327.
- [16] S. Menuel, B. Léger, A. Addad, E. Monflier, F. Hapiot, *Green Chem.* **2016**, *18*, 5500.
- [17] F. Hapiot, H. Bricout, S. Menuel, S. Tilloy, E. Monflier, *Catal. Sci. Technol.* **2014**, *4*, 1899.
- [18] F. Hapiot, E. Monflier, *Catalyst* **2017**, *7*, 173.
- [19] Y. Liu, H. Guan, J. Zhang, Y. Zhao, J.-H. Yang, B. Zhang, *Int. J. Hydrogen Energy* **2018**, *43*, 2754.
- [20] Y. Liu, J. Zhang, H. Guan, Y. Zhao, J.-H. Yang, B. Zhang, *Appl. Surf. Sci.* **2018**, *427*, 106.
- [21] A. Maleki, Z. Hajizadeh, R. Firouzi-Haji, *Microporous Mesoporous Mater.* **2018**, *259*, 46.
- [22] N. Sahiner, S. Butun Sengel, *Fuel Sci. Technol.* **2017**, *158*, 1.
- [23] S. Sadjad, M. M. Heravi, M. Malmir, *Carbohydr. Polym.* **2018**, *186*, 25.
- [24] S. Sadjad, M. Atai, *Appl. Clay Sci.* **2018**, *153*, 78.

- [25] M. Massaro, V. Schembri, V. Campisciano, G. Cavallaro, G. Lazzara, S. Milioto, R. Noto, F. Parisi, S. Riela, *RSC Adv.* **2016**, *6*, 55 312.
- [26] P. Pasbakhsh, G. J. Churchman, *Natural Mineral Nanotubes: Properties and applications*, Apple Academic Press, Oakville **2015**.
- [27] M. Massaro, G. Lazzara, S. Milioto, R. Noto, S. Riela, *J. Mater. Chem. B* **2017**, *5*, 2867.
- [28] M. Massaro, C. G. Colletti, G. Lazzara, S. Milioto, R. Noto, S. Riela, *J. Mater. Chem. A* **2017**, *5*, 13 276.
- [29] J. Tully, R. Yendluri, Y. Lvov, *Biomacromolecules* **2016**, *17*, 615.
- [30] Y. Zhang, A. Tang, H. Yang, J. Ouyang, *Appl. Catal. A* **2016**, *119*, 8.
- [31] G. Cavallaro, G. Lazzara, S. Milioto, F. Parisi, *Chem. Rec.* **2018**, *18*, 1.
- [32] P. Yuan, D. Tan, F. Annabi-Bergaya, *Appl. Clay Sci.* **2015**, *112–113*, 75.
- [33] Y. Zhang, A. Tang, H. Yang, J. Ouyang, *Appl. Clay Sci.* **2016**, *119*, 8.
- [34] J. Zhang, D. Zhang, A. Zhang, Z. Jia, D. Jia, *Iran Polym. J.* **2013**, *22*, 501.
- [35] B. Szczepanik, P. Rogala, P. M. Słomkiewicz, D. Banaś, A. Kubala-Kukuś, L. Stabrawa, *Appl. Clay Sci.* **2017**, *149*, 118.
- [36] B. Szczepanik, P. Słomkiewicz, *Appl. Clay Sci.* **2016**, *124–125*, 31.
- [37] R. Zhai, B. Zhang, L. Liu, Y. Xie, H. Zhang, J. Liu, *Catal. Commun.* **2010**, *12*, 259.
- [38] S. Kumar-Krishnan, A. Hernandez-Rangel, U. Pal, O. Ceballos-Sanchez, F. J. Flores-Ruiz, E. Prokhorov, O. Arias de Fuentes, R. Esparza, M. Meyyappan, *J. Mater. Chem. B* **2016**, *4*, 2553.
- [39] D. Tan, P. Yuan, F. Annabi-Bergaya, D. Liu, L. Wang, H. Liu, H. He, *Appl. Clay Sci.* **2014**, *96*, 50.
- [40] N. Sabbagh, A. Akbari, N. Arsalani, B. Eftekhari-Sis, H. Hamishekar, *Appl. Clay Sci.* **2017**, *148*, 48.
- [41] X. Lin, X. Ju, R. Xie, M. Jiang, J. Wei, L. Chu, *Chin. J. Chem. Eng.* **2013**, *21*, 991.
- [42] M. A. Bonifacio, G. P. A. M. Ferreira, S. Cometa, E. De Giglio, *Carbohydr. Polym.* **2017**, *163*, 280.
- [43] S. Azmi, S. I. Abd Razak, M. R. Abdul Kadir, N. Iqbal, R. Hassan, N. H. Mat Nayan, A. H. Abdul Wahab, S. Shaharuddin, *Soft Mat.* **2017**, *15*, 45.
- [44] S. Sadjad, *Appl. Organomet. Chem.* **2017**, *32*. <https://doi.org/10.1002/aoc.4211>
- [45] H. Zhu, M. L. Du, M. L. Zou, C. S. Xu, Y. Q. Fu, *Dalton Trans.* **2012**, *41*, 10 465.
- [46] P. Yuan, P. D. Southon, Z. Liu, M. E. R. Green, J. M. Hook, S. J. Antill, C. J. Kepert, *J. Phys. Chem. C* **2008**, *112*, 15 742.
- [47] S. Mallik, S. S. Dash, K. M. Parida, B. K. Mohapatra, *J. Colloid Interface Sci.* **2006**, *300*, 237.
- [48] S. Bordeepong, D. Bhongsuwan, T. Pungrassami, T. Bhongsuwan, *Songklanakarin J. Sci. Technol.* **2011**, *33*, 599.
- [49] L. Zatta, J. E. F. da Costa Gardolinski, F. Wypych, *Appl. Clay Sci.* **2011**, *51*, 165.

SUPPORTING INFORMATION

Additional supporting information may be found online in the Supporting Information section at the end of the article.

How to cite this article: Sadjadi S, Atai M. Palladated halloysite hybridized with photopolymerized hydrogel in the presence of cyclodextrin: An efficient catalytic system benefiting from nanoreactor concept. *Appl Organometal Chem.* 2019;e4776. <https://doi.org/10.1002/aoc.4776>